

Supporting Information for:

Tuning the Active Phase and Surface Chemistry of a CO₂ Hydrogenation Co/TiO₂ Catalyst with UV Light

D.N. Maaskant,¹ P.T. Prins,¹ N. S. Genz,² B. M. Weckhuysen,¹ M. Monai^{1,*}

¹Inorganic Chemistry and Catalysis, Institute for Sustainable and Circular Chemistry, Department of Chemistry, Faculty of Science, Utrecht University, Universiteitsweg 99, 3584 CG Utrecht, The Netherlands

²Paul Scherrer Institute, PSI Center for Energy and Environmental Sciences, CH-5232, Villigen PSI, Switzerland

*To whom correspondence should be addressed: m.monai.uu.nl

Contents:

- Figure S1 | Transmission *electron* microscopy-energy dispersive X-ray spectroscopy (TEM-EDX)
- Figure S2 | Catalyst characterization
- Figure S3 | Temperature programmed reduction profiles normalized to cobalt weight fitted with Gaussian functions
- Figure S4 | The effect of light on the particle size
- Figure S5 | Selectivity towards CH₄ and CO as a function of temperature, with and without illumination
- Figure S6 | Full range of the diffuse reflectance infrared spectra, as shown in Figure 5 in the main text
- Figure S7 | Diffuse reflectance infrared spectra from duplo experiment of Figure 5 in the main text
- Figure S8 | The influence of emotivities on temperature differences observed using the IR heat camera
- Table S1 | Summary of physicochemical properties of Co/TiO₂ catalyst batches and their use in experiments
- Table S2 | Results of linear combination fitting of the X-ray absorption spectroscopy (XAS) data
- Table S3 | Calibration of emissivity value for IR heat camera measurements, and sensitivity analysis thereof

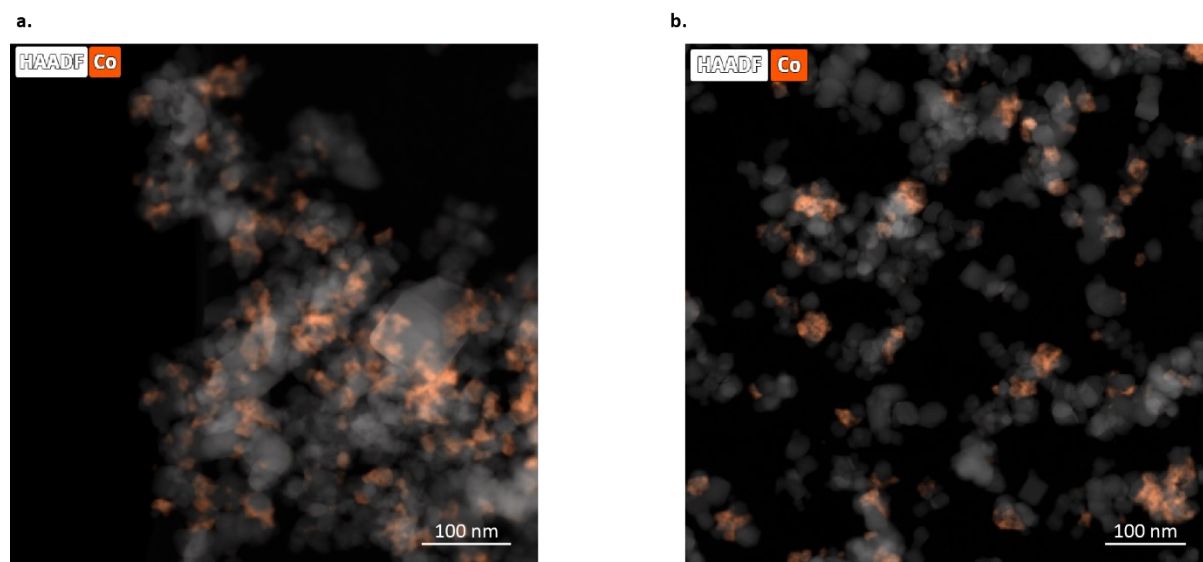


Figure S1 | Transmission electron microscopy-energy dispersive X-ray (TEM-EDX) data of the Co/TiO₂ catalyst (**a.** 6.7 wt% and **b.** 8.7 wt%).

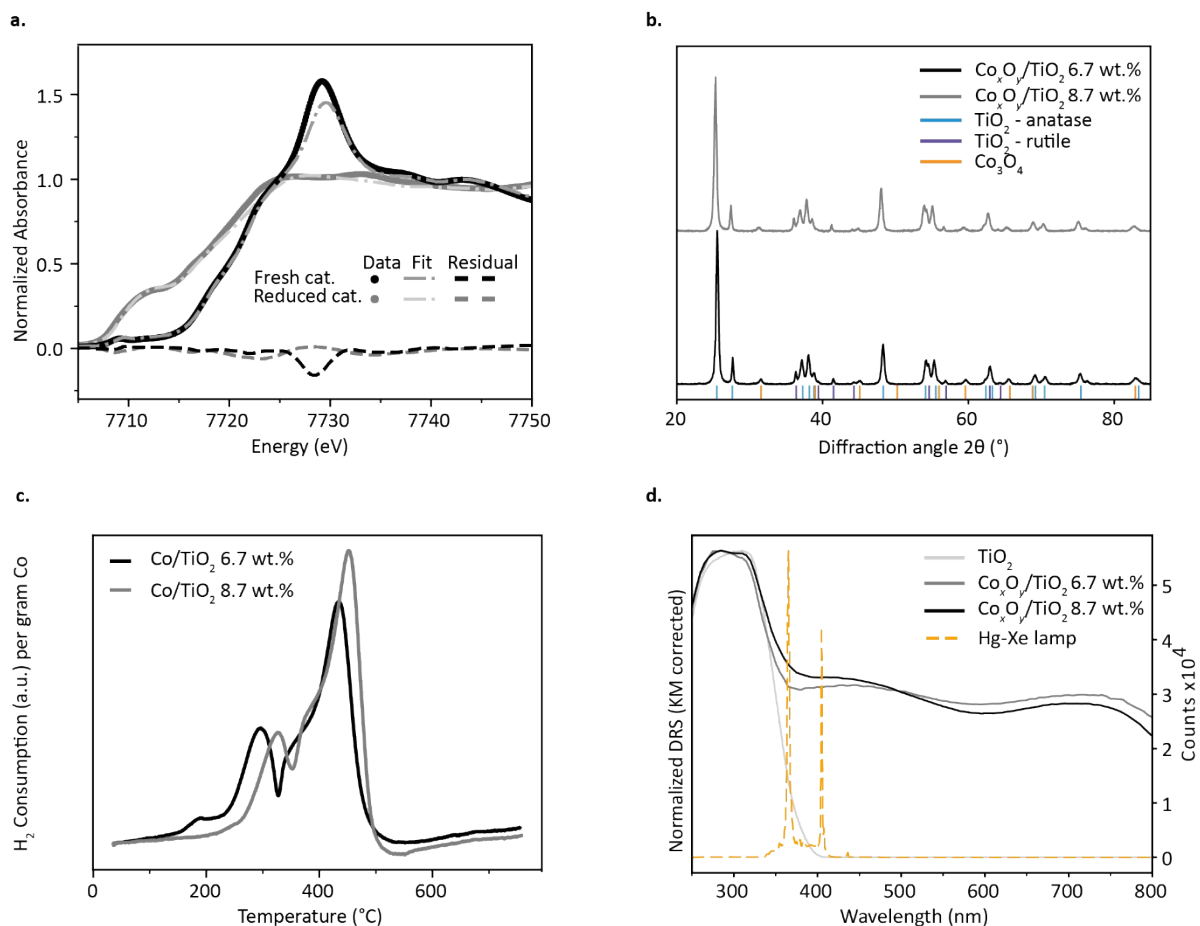


Figure S2 | **a.** X-ray absorption spectroscopy (XAS) data of the 6.7 wt% Co/TiO₂ catalyst prior to and after reduction at 450 °C (1:1=N₂:H₂, 40 mL/min, GHSV of 1 · 10⁵ h⁻¹). **b.** Normalized X-ray diffraction pattern of the Co/TiO₂ catalysts after calcination. **c.** Temperature programmed reduction (TPR) profile of the Co/TiO₂ catalysts. **d.** UV-vis diffuse reflectance spectroscopy (DRS) data of the Co/TiO₂ catalysts after calcination and TiO₂. The intensity spectrum of the Hg-Xe lamp with filter in place showing the 365 and 405 nm peaks of mercury (in yellow).

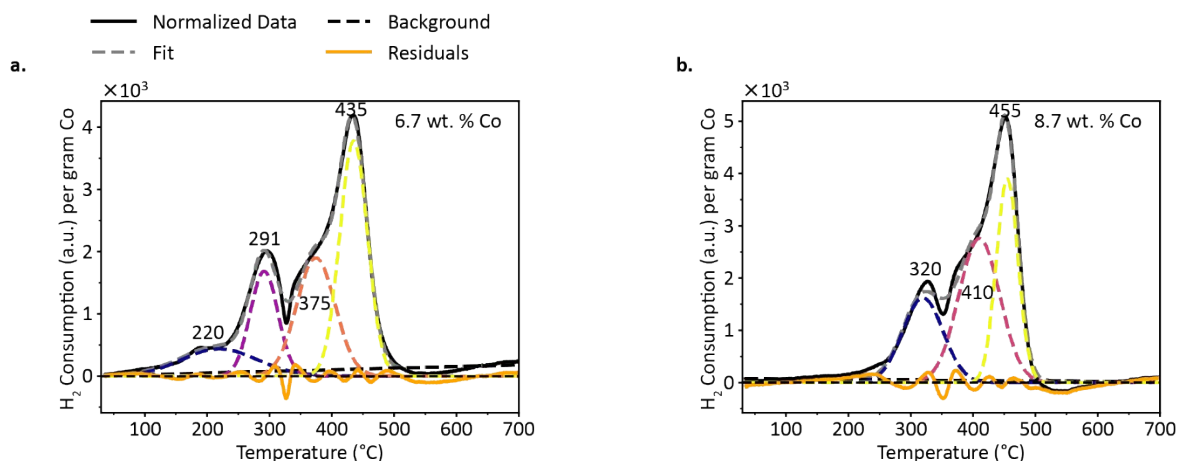


Figure S3 | Temperature programmed reduction profiles normalized to the cobalt weight fitted with Gaussian functions for the Co/TiO₂ catalysts with weight percentages of **a.** 6.7 wt.% and **b.** 8.7 wt.% Co. To compare the reducibility of both catalyst batches, we normalized the temperature programmed reduction profiles with respect to cobalt weight and fitted the peaks using Gaussian functions (Figure S3). Note that the first peak in the TPR profile of the 6.7 wt% Co/TiO₂ catalyst is an artifact due to baseline shift which appears across diverse catalyst systems without chemical justification and was therefore excluded from our analysis. The reduction peaks found by fitting are at 291, 375 and 435 °C for the 6.7 wt.% Co/TiO₂ catalyst and 320, 410 and 455 °C for the 8.7 wt.% Co/TiO₂ catalyst. The relative areas of the peaks from lowest to highest temperature are 21, 32 and 47 % for the 6.7 wt.% Co/TiO₂ catalyst and 25, 43 and 32 % for 8.7 wt.% Co/TiO₂ catalyst. The difference between batches suggests a different distribution of oxidation states before reduction, which might be a result of slight variations in flow and/or temperature during calcination. Although moderate differences exist in the temperature-programmed reduction profiles, the pre-treatment conditions (450°C for 1 h) were selected to result in a comparable reduction of the catalyst materials.

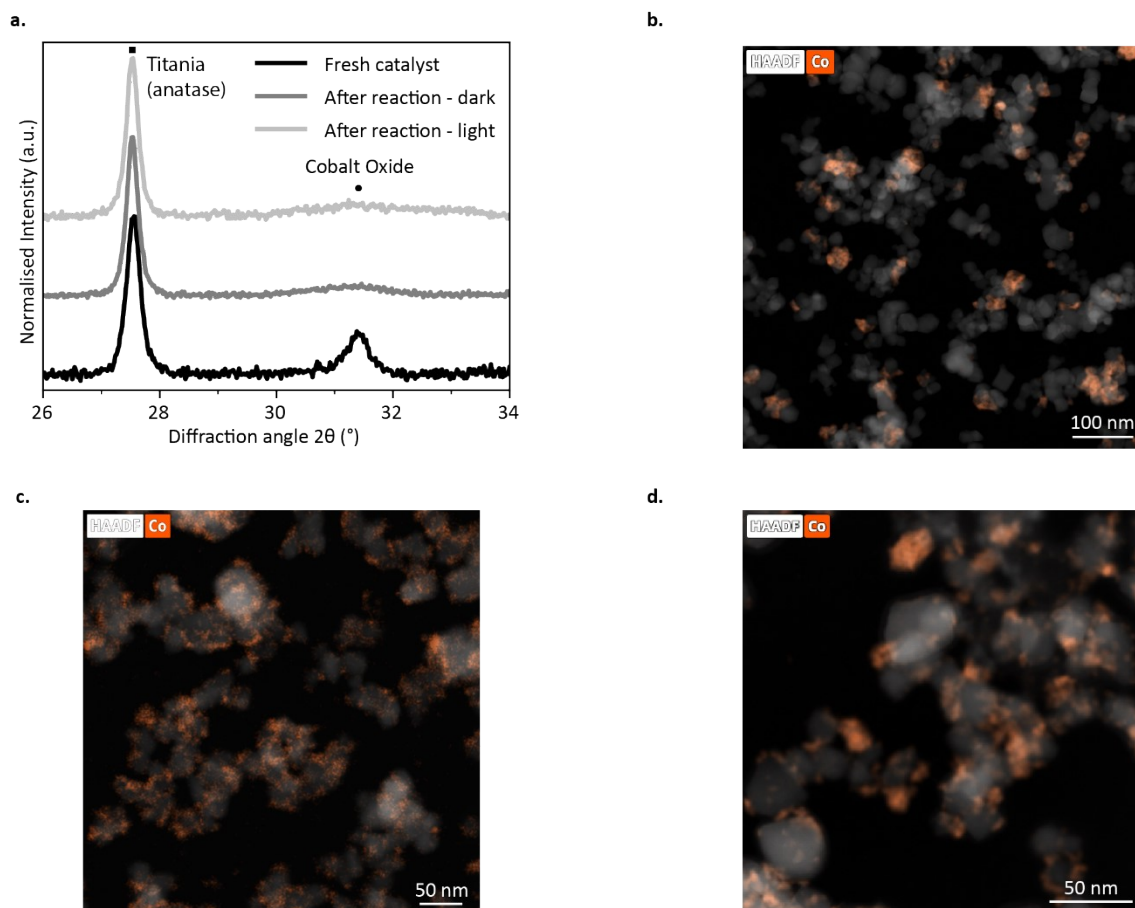


Figure S4 | The effect of light on the particle size. 8.7 wt.% **a.** XRD, and STEM-EDX of **b.** fresh, **c.** spent after reaction in the dark and **d.** spent after reaction under illumination, respectively. The spent catalysts used are the same ones used for the experiments as shown in Figure 6 (duplo) after 10 h of reaction.

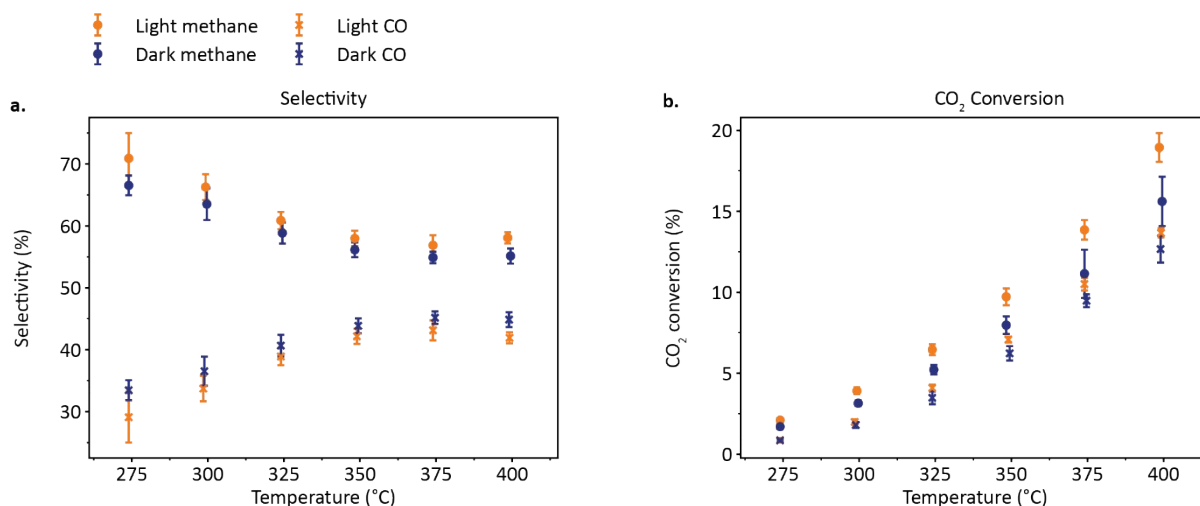


Figure S5 | Selectivity towards CH₄ and CO as a function of temperature, with and without illumination. Selectivity towards a. CH₄ and CO and b. CO₂ conversion for CO₂ hydrogenation over a 6.7 wt.% Co/TiO₂ catalyst with and without illumination (the used dataset is from the same experiments as Figure 4 in main text). Selectivity values were calculated from gas chromatographs where the integrated CO and CH₄ peak areas exceeded the limit of detection (3 σ). The limit was defined as three times the standard deviation of the CO and CH₄ peaks in blank chromatographs (10 peaks each). Conditions: The irradiance used was 130 mW/cm² (Hg-Xe lamp). The flow used was 40 mL/min, with a ratio of CO₂:H₂:He=4:16:20, and a gas hourly space velocity of 2.1 · 10⁵ h⁻¹ and 1.5 · 10⁵ h⁻¹ for with and without illumination, respectively.

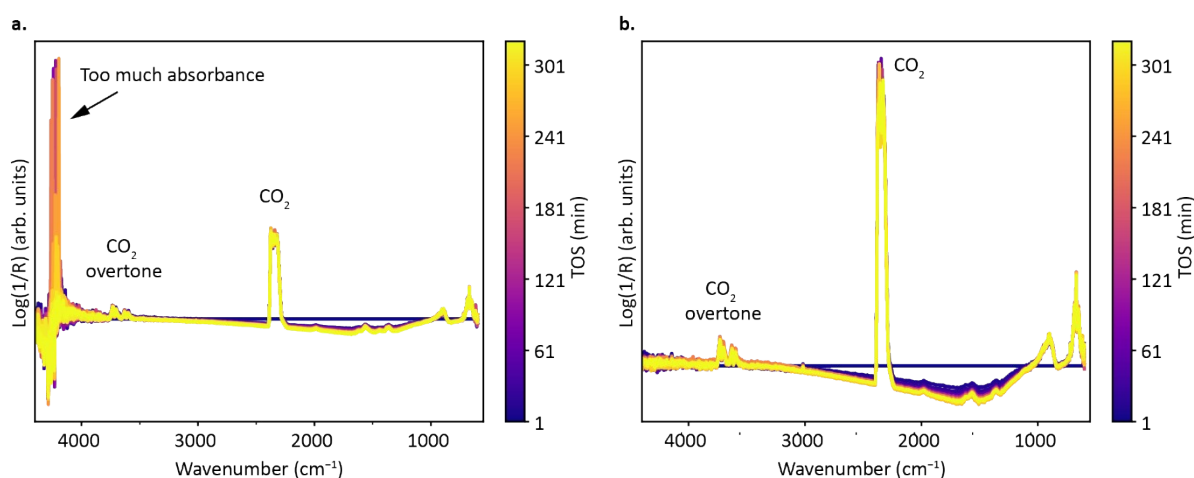


Figure S6 | Full range of the diffuse reflectance infrared Fourier transform spectroscopy (DRIFTS) data, as shown in Figure 5 in the main text with a. and b. corresponding to dark and light conditions, respectively. They were taken during CO₂ hydrogenation reaction over an 8.7 wt.% Co/TiO₂ catalyst over time (dark vs. light, respectively). Conditions: The irradiance used was 208 mW/cm² (Hg-Xe lamp). The flow used was 40 mL/min, with a ratio of CO₂:H₂:N₂=4:16:20, and a gas hourly space velocity (GHSV) of 2 · 10⁵ h⁻¹.

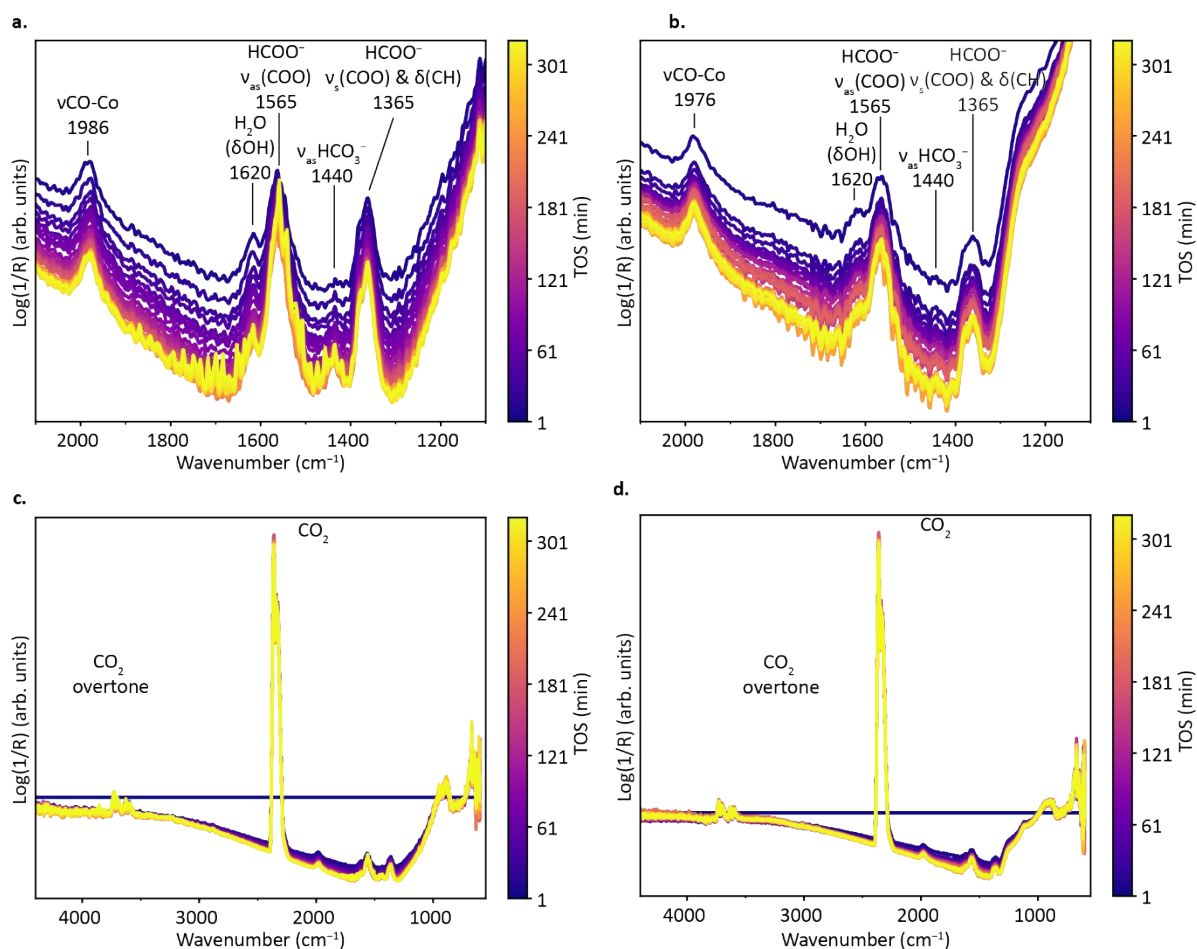


Figure S7 | **a.** and **b.** diffuse reflectance infrared Fourier transform spectroscopy (DRIFTS) data taken during the CO_2 hydrogenation reaction over a Co/TiO_2 catalyst (8.7 wt. %) with increasing time-on-stream (TOS), dark vs. light, respectively (duplo in Figure 6 of the main text). **c.** and **d.** full range of DRIFTS data in dark and under UV illumination, respectively. Conditions: The irradiance used was $208 \text{ mW}/\text{cm}^2$ (Hg-Xe lamp). The flow used was $40 \text{ mL}/\text{min}$, with a ratio of $\text{CO}_2:\text{H}_2:\text{He}=4:16:20$, and a gas hourly space velocity (GHSV) of $2 \cdot 10^5 \text{ h}^{-1}$.

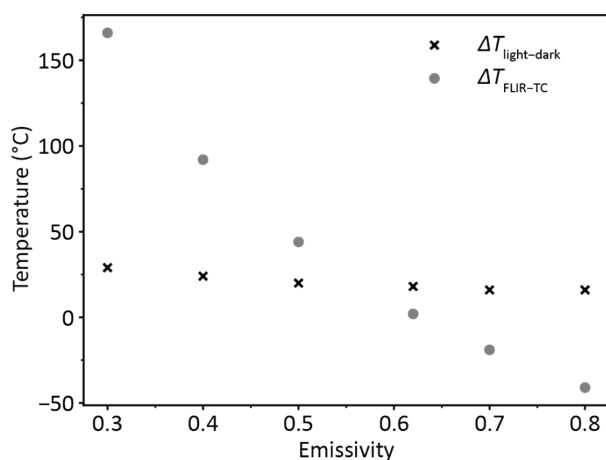


Figure S8 | **The influence of emissivities on temperature differences observed using the IR heat camera:** The temperature differences between the temperature given by the FLIR IR heat camera (T_{FLIR} with the thermocouple (T_{TC}) as function of emissivity, and between the temperature given by the FLIR IR heat camera in the dark and under illumination.

Table S1 | Summary of physicochemical properties of the two Co/TiO₂ batches (named by their weight percentages) and indication which batch was used for each experiment in this work.

	Catalyst 1 - 8.7 wt.%	Catalyst 2 - 6.7 wt.%
Temperature programmed reduction peaks (°C)	~ 320 & 455 (including shoulder)	~ 291 & 435 (including shoulder)
Pore size (cm³/g)	0.254	0.252
BET Surface Area (m²/g)	45.44	46.36
Experiments corresponding to Figure(s) and Table(s)	1, 3, 5, 6, 7, 8, S1, S2, S3, S4, S6, S7	2, 4, S1, S2, S3, S5, S8, Table 1, Table S2, Table S3

Table S2 | Linear combination fitting results for the X-ray Absorption Spectroscopy (XAS) data. The percentages of Co₃O₄, CoO and Co in the 6.7 wt% Co/TiO₂ catalyst prior to and after reduction at 450 °C (1:1=N₂:H₂, 40 mL/min and a gas hourly space velocity of 1 · 10⁵ h⁻¹) are shown.

	Fresh catalyst	Reduced catalyst
Co₃O₄ (%)	86 ± 0.8	0 ± 0.6
CoO (%)	14 ± 1.1	13 ± 0.7
Co (%)	0 ± 0.7	87 ± 0.5
R factor	4 · 10 ⁻³	2 · 10 ⁻³

Table S3 | Calibration of emissivity value for IR heat camera measurements and sensitivity analysis thereof. The catalyst temperature was measured with an internal thermocouple to be 300 °C (T_{TC}). The emissivity value was set to 0.3 to 0.9, and the apparent temperature recorded for dark and light. An emissivity value of 0.62 was selected because it resulted in the lowest difference between the temperature measured with the thermocouple and the IR camera. The difference in temperature measured with the IR heat camera between light and dark at each emissivity value is also reported to show the sensitivity of the result on the chosen emissivity value. In the emissivity calibration procedure, we assume that the temperature read by the internal thermocouple under dark is comparable to the surface temperature of the catalyst bed. However, due to gas circulation, the actual surface temperature is expected to be lower than the thermocouple reading. This discrepancy introduces a systematic error: the set emissivity value represents a lower bound, while the temperature value represents an upper bound relative to the true values. Notably, temperature gradients of 20 °C and 40 °C between the thermocouple and the surface under dark conditions would yield emissivity values of 0.7 and 0.8, respectively. Despite these high gradients, the measured temperature difference between dark and light conditions—observed using the FLIR camera—remains small, varying by only 2 °C (e.g., 18 °C vs. 16 °C for emissivity values of 0.62 and 0.8).

Emissivity	FLIR T_{dark} (°C)	$\Delta T_{\text{FLIR-TC}}$ (°C)	FLIR T_{light} (°C)	$\Delta T_{\text{light-dark}}$ (°C)
0.3	466	166	495	29
0.4	392	92	416	24
0.5	344	44	364	20
0.62	302	2	320	18
0.7	281	-19	297	16
0.8	259	-41	275	16
0.9	242	-58	256	14